Metabolism Clinical and Experimental 99 (2019) 45–56

Contents lists available at ScienceDirect

Metabolism Clinical and Experimental

journal homepage: www.metabolismjournal.com

TGR5 agonist ameliorates insulin resistance in skeletal muscles and improves glucose homeostasis in diabetic mice

Suling Huang [1], Shanyao Ma [1], Mengmeng Ning, Wenji Yang, Yangliang Ye, Lina Zhang, Jianhua Shen *, Ying Leng *

State Key Laboratory of Drug Research, Shanghai Institute of Materia Medica, Chinese Academy of Sciences, 555 Zu Chong Zhi Road, Shanghai, 201203, China

ARTICLE INFO

Article history:
Received 13 March 2019
Accepted 3 July 2019

Keywords:
TGR5
Glucose homeostasis
Insulin resistance
Skeletal muscle
Type 2 diabetes

ABSTRACT

Background and purpose: TGR5 plays an important role in many physiological processes. However, the functions of TGR5 in the regulation of the glucose metabolism and insulin sensitivity in the skeletal muscles have not been fully elucidated. We synthesized MN6 as a potent and selective TGR5 agonist. Here, the effect of MN6 on insulin resistance in skeletal muscles was evaluated in diet-induced obese (DIO) mice and C2C12 myotubes, and the underlying mechanisms were explored.

Methods: The activation of MN6 on human and mouse TGR5 was evaluated by a cAMP assay in HEK293 cell lines stable expressing hTGR5/CRE or mTGR5/CRE cells. GLP-1 secretion was measured in NCI-H716 cells and CD1 mice. The acute and chronic effects of MN6 on regulating metabolic abnormalities were observed in *ob*/*ob* and DIO mice. 2-deoxyglucose uptake was examined in isolated skeletal muscles. Akt phosphorylation, glucose uptake and glycogen synthesis were examined to assess the effects of MN6 on palmitate-induced insulin resistance in C2C12 myotubes.

Results: MN6 potently activated human and mouse TGR5 with EC_{50} values of 15.9 and 17.9 nmol/L, respectively, and stimulated GLP-1 secretion in NCI-H716 cells and CD1 mice. A single oral dose of MN6 significantly decreased the blood glucose levels in *ob*/*ob* mice. Treatment with MN6 for 15 days reduced the fasting blood glucose and HbA1c levels in *ob*/*ob* mice. MN6 improved glucose and insulin tolerance and enhanced the insulin-stimulated glucose uptake of skeletal muscles in DIO mice. The palmitate-induced impairment of insulin-stimulated Akt phosphorylation, glucose uptake and glycogen synthesis in C2C12 myotubes could be prevented by MN6. The effect of MN6 on palmitate-impaired insulin-stimulated Akt phosphorylation was abolished by siRNA-mediated knockdown of TGR5 or by the inhibition of adenylate cyclase or protein kinase A, suggesting that this effect is dependent on the activation of TGR5 and the cAMP/PKA pathway.

Conclusions: Our study identified that a TGR5 agonist could ameliorate insulin resistance by the cAMP/PKA pathway in skeletal muscles; this uncovered a new effect of the TGR5 agonist on regulating the glucose metabolism and insulin sensitivity in skeletal muscles and further strengthened its potential value for the treatment of type 2 diabetes.

1. Introduction

TGR5 is a member of the G-protein-coupled receptor (GPCR) superfamily identified in 2002 as a cell surface receptor of bile acids. It is expressed in multiple tissues, such as the gallbladder, placenta, spleen, intestines, skeletal muscles and brown adipose tissues, but the expression levels vary between different tissues [1,2]. The activation of TGR5 triggers the increase of intracellular cyclic AMP, leading to diverse downstream actions, and TGR5 participates in a large spectrum of biological processes, such as anti-inflammation, gallbladder relaxation, intestinal motility, glucose homeostasis and energy metabolism [3–5]. The overexpression of TGR5 could ameliorate glucose intolerance in high-fat diet-induced obese (DIO) mice by stimulating GLP-1 secretion and insulin release in response to glucose loading, while the knockdown of TGR5 exacerbates glucose intolerance [6,7]. The TGR5 agonists, such as INT-777 and TRC210258, could significantly prevent obesity and insulin resistance in DIO mice [6,8]. RDX8940, a novel intestinal TGR5 agonist, improved liver steatosis and insulin sensitivity in mice fed a

Abbreviations: AC, adenylate cyclase; cAMP, cyclic adenosine monophosphate; DIO, diet induced obesity; DPP-4, dipeptidyl peptide 4; EDL, extensor digitorum longus; FXR, farnesoid X receptor; GLP-1, glucagonlike peptide-1; HFD, high-fat diet; ITT, insulin tolerance test; LCA, lithocholic acid; OGTT, oral glucose tolerance test; PKA, protein kinase A; TGR5, Takeda G-protein-coupled receptor 5; UCP1, uncoupling protein 1.

* Corresponding authors at: State Key Laboratory of Drug Research, Shanghai Institute of Materia Medica, Chinese Academy of Sciences, Zu Chong Zhi Road 555, Shanghai, 201203, China.
E-mail addresses: jhshen@simm.ac.cn (J. Shen), yleng@simm.ac.cn (Y. Leng).

[1] The first two authors contributed equally to this work.

https://doi.org/10.1016/j.metabol.2019.07.003
0026-0495/

Western diet [9]. This evidence suggests that TGR5 is an attractive target for the treatment of metabolic diseases.

Currently, the main superiority of TGR5 for treating diabetes is based on its two physiological effects. One is that the activation of TGR5 in intestinal enteroendocrine cells will evoke the release of GLP-1, an insulinotropic hormone that regulates insulin and glucagon secretion along with gastrointestinal motility and appetite [10–12]. Another is the activation of TGR5 in brown adipose tissue and the muscles will induce the expression of mitochondrial uncoupling protein 1 (UCP1) and D2 (type 2 deiodinase), promotes intracellular thyroid hormone activation and induces energy expenditure [5,13]. As an important insulin target tissue, the skeletal muscle plays a key role in glucose disposal. Insulin resistance in the skeletal muscle resulted in a decrease in insulin-stimulated glucose transport and glycogen synthesis [14,15], thus impairing the whole-body glucose homeostasis [16–18]. TGR5 activation promotes GLP-1 secretion and subsequently improves the whole-body glucose homeostasis and insulin sensitivity, which may indirectly lead to the amelioration of insulin resistance in skeletal muscles [19]. Although some direct effects of TGR5 activation on skeletal muscle were reported to increase the D2 expression and activity and to enhance oxygen consumption [5,20], the molecular functions of TGR5 activation in skeletal muscle are still far from being elucidated. A recent study found that the exercise-induced unfolded protein response could increase TGR5 expression and could thus promote skeletal muscle cell differentiation in mice [21]. However, the direct regulation of TGR5 activation on glucose metabolism and insulin signaling in skeletal muscle has not been fully investigated. We wondered whether the activation of TGR5 in skeletal muscles may affect insulin signaling and if it could correct insulin resistance in type 2 diabetes.

We developed and synthesized a series of potent and selective TGR5 agonists [22–26], and MN6 (compound 22 g in reference 26) was a representative compound that activated both human and mouse TGR5 with EC_{50} values of 1.5 nmol/L and 18 nmol/L, respectively, and did not activate FXR [26]. In the present study, the stimulation of GLP-1 secretion and the antihyperglycemic effect of MN6 were evaluated both in vitro and in vivo using *ob*/*ob* and DIO mice, which are well-established, clinically relevant models of diabesity [27,28]. More importantly, by utilizing MN6 as a potent and selective TGR5 agonist, we demonstrated the beneficial effects of TGR5 in the amelioration of insulin resistance in the skeletal muscles of DIO mice and C2C12 myotubes and further explored the underlying mechanisms.

2. Materials and methods

2.1. Materials

MN6 was synthesized as described [26]. BI1356 and LCA were purchased from Kaifang Pharmaceutical Technology Co. Ltd. (Shanghai, China) and TCIChemical Industry Development Co., Ltd. (Shanghai, China), respectively. The adenylate cyclase (AC) inhibitor MDL-12330-A hydrochloride and the protein kinase A (PKA) inhibitor H89 were purchased from Sigma Aldrich (St. Louis, MO, USA). The polyvinylidene difluoride membranes were purchased from Merck Millipore (Bedford, MA, USA). The primary antibodies against phospho-Akt (Ser473) (#9271L), phospho-Akt (Thr308) (#9275L), pan-Akt (#9272S) and GAPDH (#2118L) were obtained from Cell Signaling Technology (Beverly, MA, USA). The horseradish peroxidase-conjugated secondary antibody and siLentFect lipid were purchased from Bio-Rad (Shanghai, China). The 1,2-deoxy-D-[1,2-^{3}H] glucose and D-[U-^{14}C] glucose were purchased from PerkinElmer (Massachusetts, USA). The siRNA-targeted TGR5 was purchased from Dharmacon RNA Technology (Lafayette, CO, USA). The Universal SYBR Green Supermix and 96-well optical reaction plates were separately purchased from TaKaRa (Dalian, China) and BIOplastics (Rötscherweg, Netherlands). The primers were synthesized by Invitrogen (Shanghai, China).

2.2. Animals

CD1 mice and C57BL/6J mice were purchased from SLAC Laboratory Animals (Shanghai, China). B6.V-*Lep^{ob}*/*Lep^{ob}* mice (Jackson Laboratory, Bar Harbor, ME, USA) were bred at the Shanghai Institute of Materia Medica Chinese Academy of Sciences (Shanghai, China). All mice were housed in a specific, pathogen-free class laboratory and were maintained at a controlled room temperature (22–24 °C) under a 12 h light-dark cycle with free access to water and food. For the DIO mouse study, C57BL/6 J male mice were fed a high-fat diet (60 kcal% fat, 20 kcal% protein and 20 kcal% carbohydrate; Cat. D12492i, Research Diet, New Brunswick, NJ, USA). The animal experiments were conducted in accordance with the guides by the Institutional Animal Care and Utilization Committee (IACUC) of Shanghai Institute of Materia Medica (SIMM), Chinese Academy of Sciences (CAS). The protocol was approved by the IACUC, SIMM, CAS.

2.3. In vitro TGR5 assay

Human or mouse TGR5/CRE/HEK293 stable cell lines were obtained and maintained as described [26]. MN6 was diluted into different concentrations and was used to treat cells for 0.5 h. The intracellular cAMP production was determined by the HTRF cAMP Assay Kit (Cisbio, France).

2.4. In vitro GLP-1 assay

The assay was performed as described previously [25]. Briefly, human enteroendocrine NCI-H716 cells were washed with KREBS (NaCl 128.8 mM, KCl 4.8 mM, KH_2PO_4 1.2 mM, $MgSO_4$ 1.2 mM, $CaCl_2$ 2.5 mM, $NaHCO_3$ 5 mM and HEPES 10 mM) and then were incubated with different concentrations of MN6 in KREBS (containing 0.2% BSA and 1% DPP-4 inhibitor) for 2 h at 37 °C. GLP-1 was collected from the incubation buffer and was assayed using an Active GLP-1 ELISA Kit (Millipore, USA). The sensitivity of the GLP-1 assay was 2 pmol/L, and the intra-assay and inter-assay CVs were 2.5% and 8.4%, respectively.

2.5. GLP-1 secretion in CD1 mice

Male CD1 mice were fasted overnight and were randomly assigned to four groups (n = 9) based on their body weight. MN6 (25, 50 or 100 mg/kg) or the vehicle (0.25% CMC-Na) were orally administered to CD1 mice. Then, 1 h later, all mice were challenged with 4 g/kg glucose, and blood samples were collected 5 min after the glucose challenge began; then, the samples were placed in Eppendorf tubes containing a DPP-4 inhibitor (Millipore, DPP-4-010) with a final concentration of 1% blood samples and 25 mg/mL EDTA to measure the plasma active GLP-1[7–36 amide] levels.

Male CD1 mice were randomly assigned to eight groups (n = 10) based on their body weights (26–28 g) and were orally administered 50 mg/kg MN6, 3 mg/kg BI1356, 50 mg/kg MN6 combined with 3 mg/kg BI1356 or the vehicle (0.25% CMC-Na). All food was removed before the administration. The blood samples were collected at 4 h and 8 h after dosing as described above to measure the active GLP-1 level. The mice were kept in a fasting state during the treatment.

2.6. MN6 treatment in ob/ob mice

Seven- to eight-week-old male *ob*/*ob* mice were randomly assigned to two groups (n = 10) based on their fasting blood glucose and insulin levels and their body weights, and they were subjected to gavage treatment with 50 mg/kg MN6 or the vehicle (0.25% CMC-Na) after 2 h of fasting. The blood glucose levels were determined before dosing and 2, 4, 6, 10 and 24 h after dosing. The mice were given food again at 6 h. After that, the *ob*/*ob* mice were continuously treated with 50 mg/kg MN6 and the vehicle twice daily for 17 days. The fasting

blood glucose levels of *ob*/*ob* mice were detected on day 4, 8, 12 and 15. The food intake levels were measured daily except the days detecting fasting blood glucose. The body weights were measured every day. Blood samples were collected for HbA1c measurement on treatment day 15. These mice were euthanized by carbon dioxide asphyxiation on day 17.

2.7. Chronic MN6 administration in DIO mice

C57BL/6J male mice (3–4 weeks) were fed a formulated research diet containing 60% of the calories from fat (high-fat diet) for 16 weeks before and throughout the duration of the experiment. A corresponding group of C57BL/6 J male mice (n = 20) fed with standard diet (SD) was set. DIO mice were randomly assigned to two (n = 20) groups based on their fasting blood glucose levels and body weights and were subjected to a twice daily gavage administration of 50 mg/kg MN6 or the vehicle (0.25% CMC-Na) for 39 days. The standard diet mice were administrated by gavage with the vehicle (0.25% CMC-Na) twice daily. The fasting blood glucose levels were measured at day 12, 18 and 24 after dosing. An oral glucose tolerance test (OGTT, 1.5 g/kg glucose, n = 10) and an insulin tolerance test (ITT, 0.5 U/kg insulin, n = 10) were performed in 10 different mice randomly chosen from each group on days 28 and 35, respectively. On the last day of administration, the mice were anaesthetized with an i.p. injection of sodium pentobarbital (60 mg/kg). Eight mice from the vehicle- and MN6-treated groups were randomly selected, and the soleus and extensor digitorum longus (EDL) muscles were isolated to perform a 2-deoxyglucose uptake assessment [29,30]. Briefly, the muscles were incubated in pregassed (95% O_2/5% CO_2) KHB buffer containing 5 mmol/L glucose and 15 mM mannitol, with or without 12 nM insulin for 30 min and were then rinsed in glucose-free KHB buffer with or without insulin for 10 min; this was followed by an incubation in vials containing 1 mmol/L 2-deoxy-D-glucose, 19 mmol/L mannitol, 2.5 μCi/mL [1,2-^{3}H]-2-deoxy-D-glucose, and 0.7 μCi/mL [^{14}C] mannitol with or without insulin for 20 min. The gas phase (95% O2/5% CO_2) and temperature (30 °C) were maintained during the muscle incubation. The muscles were frozen in liquid nitrogen and were processed as described previously [29]. The glucose transport activity is expressed as glucose analogue accumulated (μmol) per milliliter of intracellular water per hour.

2.8. Protein phosphorylation, glucose uptake and glycogen synthesis in C2C12 myotubes

C2C12 myoblasts (American Type Culture Collection, ATCC) were maintained in DMEM containing 10% FBS at 37 °C and 5% CO_2. The confluent cells were differentiated into myotubes by culturing with DMEM containing 2% horse serum (HS) for 5 days. To evaluate the effects of MN6 or LCA on palmitate-induced insulin resistance, C2C12 myotubes were preincubated with or without MN6 or LCA for 8 h and were then coincubated with BSA or 0.75 mM palmitate for 16 h.

For protein phosphorylation measurements, C2C12 myotubes were pretreated as described above, and then the myotubes were homogenized and subjected to western blot analysis. The protein preparation and western blot analyses were performed as described previously [29]. The primary antibodies used in this study included anti-GAPDH (dilution 1:4000), anti-phospho-Akt (Ser 473) (dilution 1:1000), anti-phospho-Akt (Thr 308) (dilution 1:1000) and anti-pan-Akt (dilution 1:1000). The blots were blocked in 7.5% milk and were then incubated overnight at 4 °C with the primary antibody; this was followed by an incubation with the goat anti-rabbit antibody (dilution 1:10000). The blot bands were visualized via ECL plus chemiluminescence (Amersham, IL, USA) and were quantified via densitometry using Quantity One (Bio-Rad, USA).

For 2-deoxyglucose uptake, C2C12 myotubes were pretreated as described above and were then incubated in KRHB (130 mM NaCl, 5 mM KCl, 1.3 mM $MgSO_4$, 1.3 mM $CaCl_2$, 25 mM HEPES, pH 7.4) with or without 100 nM insulin for 30 min; this was followed by incubation with 0.05 mM 2-deoxy-D-glucose and 0.5 μCi/mL 2-deoxy-D-[1,2-^{3}H] glucose at 37 °C for 10 min. The glucose uptake was terminated by three quick washes with ice-cold PBS followed by the addition of 150 μL of 0.1% (vol/vol) Triton-X 100 for the quantitation of [^{3}H] using liquid scintillation. The radioactivity was determined by liquid scintillation counting (Perkin Elmer Trilu, Massachusetts, USA). The data were normalized against the protein concentration, as determined by a Bradford assay. The net insulin stimulated glucose uptake was calculated as described previously [31].

For the determination of glycogen synthesis, C2C12 myotubes were pretreated as described above and were then incubated in medium supplemented with D-[U-^{14}C] glucose (1 μCi/mL) in the presence or absence of 100 nM insulin for 1 h. The cells were lysed with 1 M NaOH, and ethanol was added to precipitate the glycogen for 2 h at 4 °C. The incorporation of [^{14}C] glucose into the glycogen was measured by liquid scintillation counting.

2.9. Transfection of TGR5 siRNA and quantitative real-time PCR

To knock down the expression of TGR5, small interfering RNAs targeting mouse TGR5 (ON-TARGETplus SMARTpool; Dharmacon RNA Technology, Lafayette, CO, USA) were transfected twice using siLentFect Lipid Reagent (Bio-Rad, CA, USA) on day 2 and day 4 during C2C12 myotube differentiation. The gene expression of TGR5 was analyzed by quantitative PCR as previously described [29] and was normalized to the expression of β-actin. The primer sequences were as follows: TGR5, TRG5F (5′-GGGTCAGCTCCCTGTTCTTT-3′), and TRG5R (5′-CAGGGTTGAGGGTACATCGC-3′); β-actin, β-actinF (5′-GTACGACCAGAGGCATACAG-3′), and β-actinR (5′-CTGAAGTAC CCCATTGAACA-3′).

2.10. Intracellular cAMP assay in C2C12 myotubes

C2C12 myotubes were treated with MN6 at the indicated concentrations for 0.5 h and were then lysed by treatment with 0.1 M HCl. The intracellular cAMP levels were measured using an ELISA kit purchased from Enzo Life Science (Farmingdale, NY, USA).

2.11. Statistical analysis

The results are expressed as the means ± SEMs. The statistical significance was determined by Student's unpaired *t*-test (two-tailed) using GraphPad Prism software. The values of $P < 0.05$ were considered statistically significant.

3. Results

3.1. MN6 is a potent TGR5 agonist that stimulates GLP-1 secretion both in vitro and in vivo

In a previous study, we reported a synthetic small molecule, MN6 (Fig. 1A), as a selective and potent TGR5 agonist with EC_{50} values of 1.5 and 18 nM on hTGR5 and mTGR5, respectively, by a CRE-driven luciferase reporter gene assay in either the hTGR5/CRE/HEK293 or mTGR5/CRE/HEK293 stable cell line [26]. Here, we detected the effects of MN6 on cAMP production in the same cell lines. As shown in Fig. 1B and C, MN6 resulted in a dose-dependent elevation of the intracellular cAMP levels in human and mouse TGR5/CRE/HEK293 stable cell lines, with an EC_{50} value of 15.9 nM on hTGR5 and 17.9 nM on mTGR5. Lithocholic acid (LCA), a natural ligand of TGR5, showed much weaker activity, with an EC_{50} value of 0.74 μM on hTGR5 and 1.64 μM on mTGR5. MN6 significantly promoted GLP-1 secretion in human enteroendocrine NCI-H716 cells in a dose-dependent manner. GLP-1 secretion was increased to 2-fold of that of the control after a 2 h

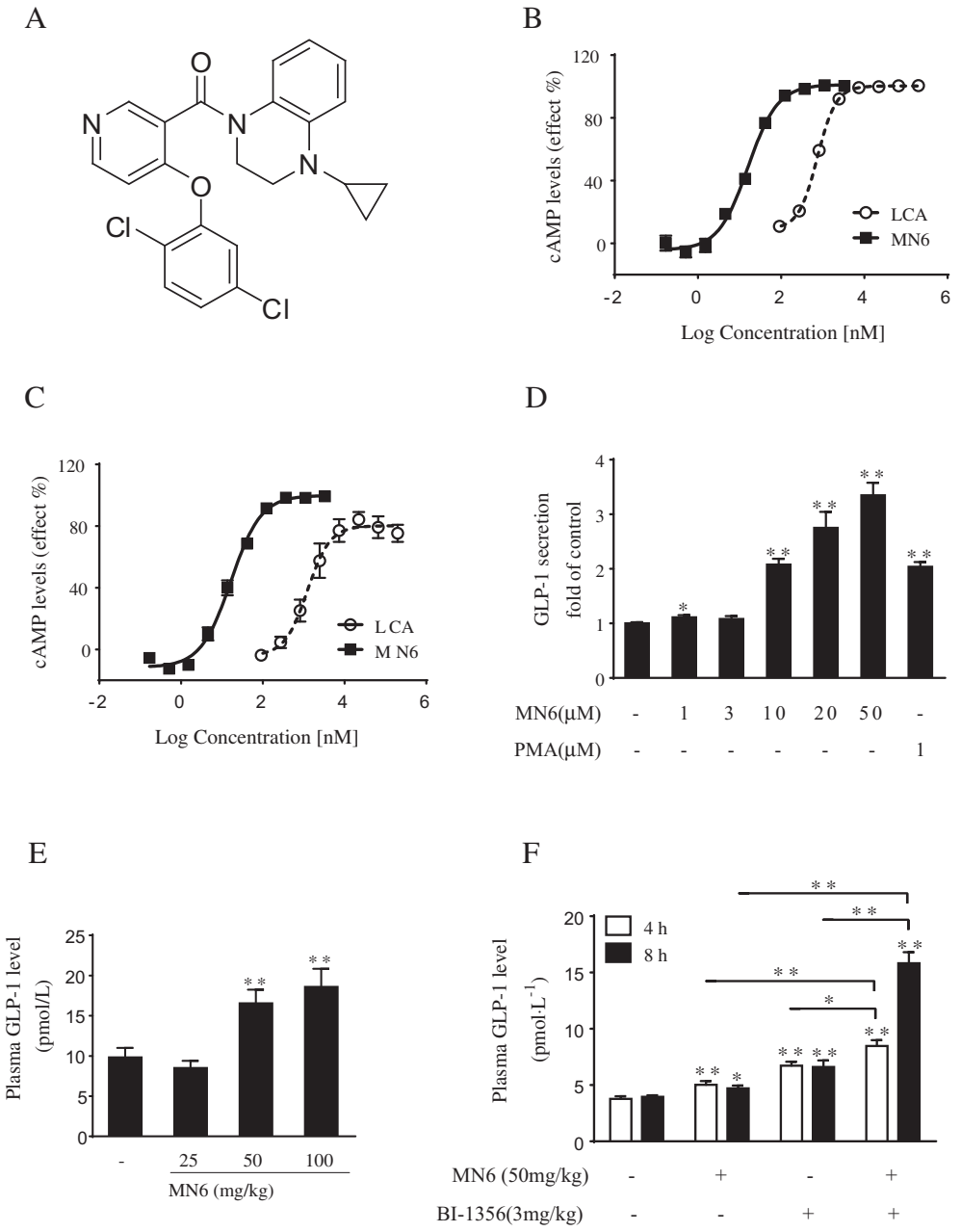

Fig. 1. MN6, a potent agonist of TGR5, increased the intracellular cAMP levels and stimulated GLP-1 secretion both in vitro and in vivo. (A) The chemical structure of MN6. (B, C) Intracellular cAMP levels in HEK293 cells transfected with a human (B) or mouse (C) TGR5 expression plasmid and a CRE-driven luciferase reporter plasmid and treated with MN6 or LCA for 0.5 h at the indicated concentrations (n = 3). (D) GLP-1 levels in NCI-H716 cells treated with MN6 for 2 h at the indicated concentrations (n = 3). (E) CD1 mice were treated with MN6 at the indicated doses 1 h prior to glucose load administration (4 g/kg), and then the blood samples were collected for plasma active GLP-1 detection 5 min after the glucose load was administered (n = 9). (F) Plasma active GLP-1 levels in CD1 mice treated with 50 mg/kg MN6, 3 mg/kg BI-1356 or cotreated with both compounds for the indicated times (n = 10). The results are expressed as the means ± SEMs. $^{*}P < 0.05$, $^{**}P < 0.01$ versus the corresponding controls or as indicated.

treatment with 10 μM MN6 (Fig. 1D). Then, we further investigated the effect of MN6 on active GLP-1 levels in vivo. MN6 increased the plasma active GLP-1 level in CD1 mice following a glucose bolus, with a 68.5% or 89.3% increase after a single dose of 50 or 100 mg/kg MN6, respectively (Fig. 1E). As GLP-1 can be degraded by DPP-4, we then tested the synergistic effect between MN6 and BI-1356, a known DPP-4 inhibitor. The results show that a single dose of either 50 mg/kg MN6 or 3 mg/kg BI-1356 significantly increased the plasma active GLP-1 levels in CD1 mice 4 h or 8 h after treatment. Cotreatment with MN6 and BI-1356 resulted in a more significant increase in the plasma active GLP-1 levels, especially at 8 h, reaching a 4-fold increase compared to that of the control (Fig. 1F).

3.2. MN6 improved glucose homeostasis in diabetic mice

In our previous study [26], MN6(22 g) showed similar EC_{50} on mTGR5 activation with 23 g, thus we using 50 mg/kg, the same dose with 23 g to investigate the efficacy of MN6 in *ob*/*ob* mice. The pharmacokinetic data of MN6 in rats and *ob*/*ob* mice were showed in Supplementary Tables 1 and 2. In *ob*/*ob* mice, a single dose of 50 mg/kg MN6 significantly reduced the blood glucose levels, with a 33.1% reduction 2 h after dosing, which was sustained and significantly lower up until 12 h after dosing (Fig. 2A). The chronic administration of 50 mg/kg MN6 to *ob*/*ob* mice for 15 days decreased the fasting blood glucose level by 32.9% on average (Fig. 2B), and the HbA1c level was reduced

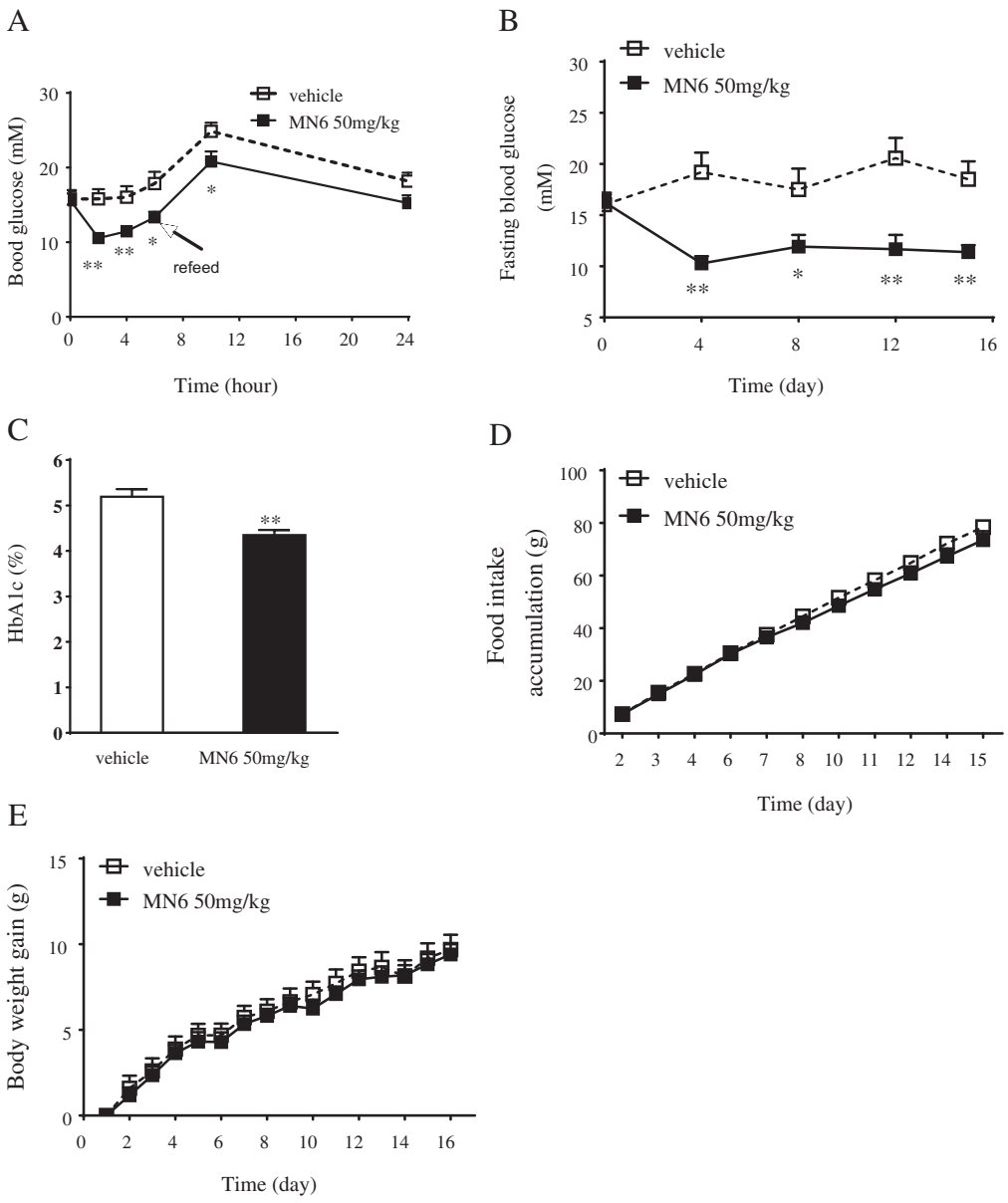

Fig. 2. MN6 improved glucose homeostasis in *ob*/*ob* mice. The blood glucose levels were measured in *ob*/*ob* mice (n = 10) (A) after a single oral treatment of MN6 at the indicated dose. For the chronic study in *ob*/*ob* mice (n = 10), the fasting blood glucose levels (B), the food intake (D) and the change in body weight (E) were measured throughout the treatment. (C) The HbA1c levels were determined on day 15 of the treatment. The results are presented as the means ± SEMs. $^{*}P < 0.05$, $^{**}P < 0.01$ versus the mice receiving the vehicle.

by 16.3% (Fig. 2C). No changes in food intake or body weight were observed during the treatment (Fig. 2D and E).

3.3. MN6 improved metabolic abnormalities and increased the insulin-stimulated glucose uptake in the skeletal muscles of DIO mice

To investigate whether MN6 could restore metabolic homeostasis in subjects who were already obese and insulin resistant, we generated DIO by feeding mice a HFD (high-fat diet) for 16 weeks. Thereafter, the mice were treated with MN6 (50 mg/kg bid) for 39 days. The HFD mice exhibited obesity, hyperglycemia, severe glucose intolerance and insulin resistance compared with the characteristics of the SD (standard diet) mice (Fig. 3A–F). MN6 significantly decreased the fasting-blood glucose level at day 18 and day 24 (Fig. 3A). During the whole treatment, MN6 induced statistically significant decreases on the body weight and food intake of DIO mice, with reductions of 11.3% (Fig. 3B) and 13.6% (Fig. 3C), respectively. After 28 days of treatment with MN6, the HFD mice exhibited a significant reduction in their blood glucose levels following an oral glucose challenge (Fig. 3D), and the mice exhibited a 22.0% reduction of the AUC (Fig. 3E). Treatment with MN6 for 35 days also evoked a significantly greater reduction in the blood glucose values at 90 and 120 min after the insulin injection, indicating improved insulin sensitivity in MN6-treated DIO mice (Fig. 3F). To further investigate the insulin sensitivity of the skeletal muscles in MN6-treated DIO mice, EDL and soleus muscles were isolated to perform 2-deoxyglucose uptake analysis. As shown in Fig. 3G and H, the insulin-stimulated glucose uptake was enhanced by 19.0% in the soleus muscle and by 19.2% in the EDL muscle, indicating an improvement in insulin sensitivity.

3.4. MN6 prevented palmitate-induced insulin resistance in C2C12 myotubes

To investigate the direct effects of MN6 on the insulin sensitivity of the skeletal muscles, we cultured C2C12 myotubes with palmitate

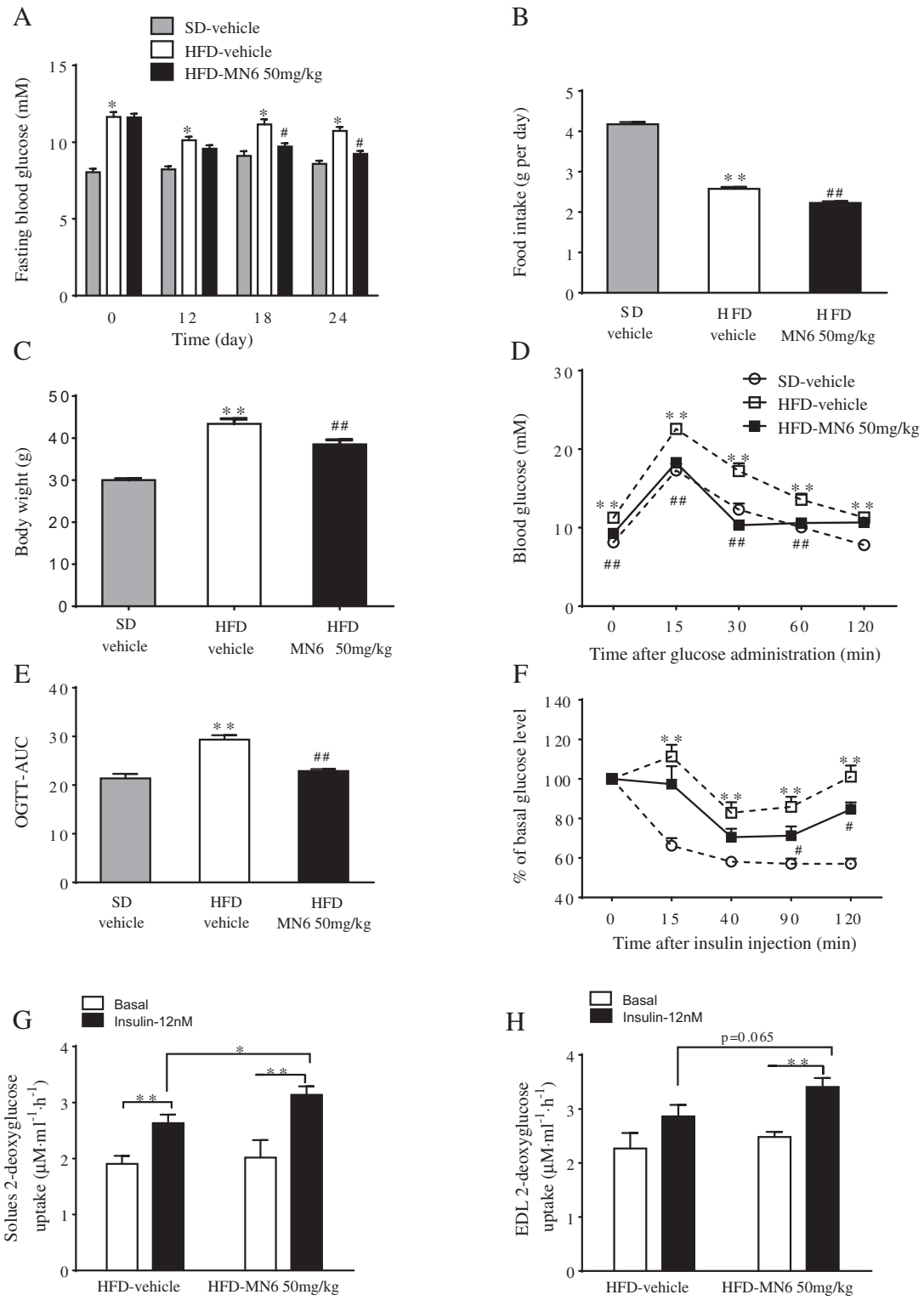

Fig. 3. MN6 lowered the blood glucose levels and improved the insulin sensitivity in DIO mice. DIO mice were treated as described in the Methods section. The fasting blood glucose levels (A), body weight (B) and food intake (C) were determined throughout the treatment (n = 20). OGTT (D and E) and ITT (F) were determined on days 28 and 35 of the treatment (n = 10), respectively. The soleus (G) and EDL (H) muscles were isolated, and 2-deoxyglucose uptake was determined under basal or insulin-stimulated (12 nmol/L) conditions (n = 7–8). SD: standard diet; HFD: high-fat diet. The results are presented as the means ± SEMs. $^{*}P < 0.05$, $^{**}P < 0.01$ versus the SD group or as indicated; $^{\#}P < 0.05$, $^{\#\#}P < 0.01$ versus HFD-vehicle group.

to induce insulin resistance. After a 16 h incubation with 0.75 mM palmitate, the C2C12 myotubes showed significant decrease in the insulin-stimulated phosphorylation of Akt (Ser 473 and Thr 308), glucose uptake and glycogen synthesis (Fig. 4). Preincubating C2C12 myotubes with 0.3 μM MN6 significantly prevented the palmitate impairment of the insulin-stimulated phosphorylation of

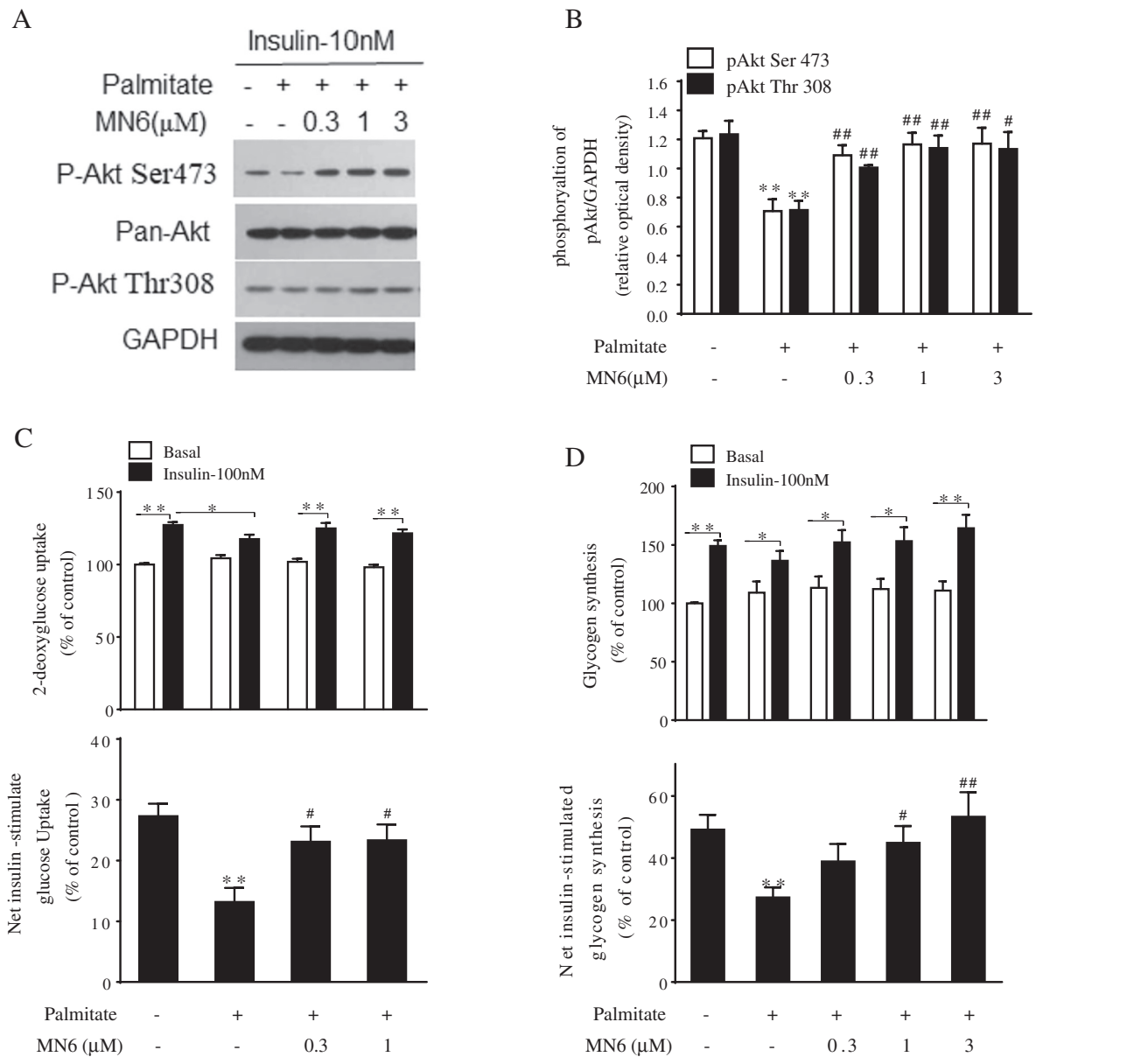

Fig. 4. MN6 prevented palmitate-induced insulin resistance in C2C12 myotubes. (A, B) C2C12 myotubes were pretreated with MN6 at the indicated concentrations for 8 h and were then coincubated with 0.75 mM palmitate for 16 h, followed by stimulation with 10 nM insulin for 30 min. The cells were collected, and the cell lysates were analyzed by western blotting using primary antibodies specific to phospho-Akt, pan-Akt and GAPDH (n = 5). (C) The C2C12 myotubes were pretreated as above, and then the glucose uptake was detected. The net insulin-stimulated glucose uptake was calculated by the value of insulin-stimulated glucose uptake minus the value of basal glucose uptake (n = 5). (D) The C2C12 myotubes were pretreated as above, and glycogen synthesis was detected. The net insulin-stimulated glycogen synthesis was calculated by the value of insulin-stimulated glycogen synthesis minus the value of basal glycogen synthesis (n = 4). The results are presented as the means ± SEMs. $^{*}P < 0.05$, $^{**}P < 0.01$ versus control group or as indicated; $^{\#}P < 0.05$, $^{\#\#}P < 0.01$ versus the palmitate-treated group.

Akt (Ser 473 and Thr 308) and glucose uptake (Fig. 4A-C). The palmitate-induced attenuation of insulin-stimulated glycogen synthesis could also be prevented by preincubation with 1 μM MN6 (Fig. 4D).

3.5. TGR5 is indispensable in the prevention of palmitate-induced insulin resistance by MN6 in C2C12 myotubes

MN6 elevated the intracellular cAMP levels in C2C12 myotubes in a dose-dependent manner (Fig. 5A). To determine whether the effects of MN6 on the cAMP levels and on the palmitate-induced impairment of insulin-stimulated Akt phosphorylation was dependent on TGR5, TGR5 expression was downregulated by siRNAs in C2C12 myotubes. After siRNA interference, the TGR5 expression was reduced to 55% of that of the negative control group (Fig. 5B). As shown in Fig. 5C, down-regulation of TGR5 completely blocked the MN6-induced elevation of the cAMP levels. Furthermore, the preventive effects of MN6 on the palmitate-induced reduction of insulin-stimulated Akt phosphorylation (Ser 473 and Thr 308) were also blocked by down-regulation of TGR5 (Fig. 5D–F). These data indicate that MN6 protected the C2C12 myotubes against palmitate-induced insulin resistance in a manner that was dependent on TGR5.

3.6. Activation of TGR5 by MN6 prevented palmitate-induced insulin resistance via the cAMP/PKA pathway in C2C12 myotubes

Since the activation of TGR5 triggered a cAMP release that may lead to the activation of protein kinase A (PKA), we further examined the involvement of cAMP and PKA in the preventative effects of MN6

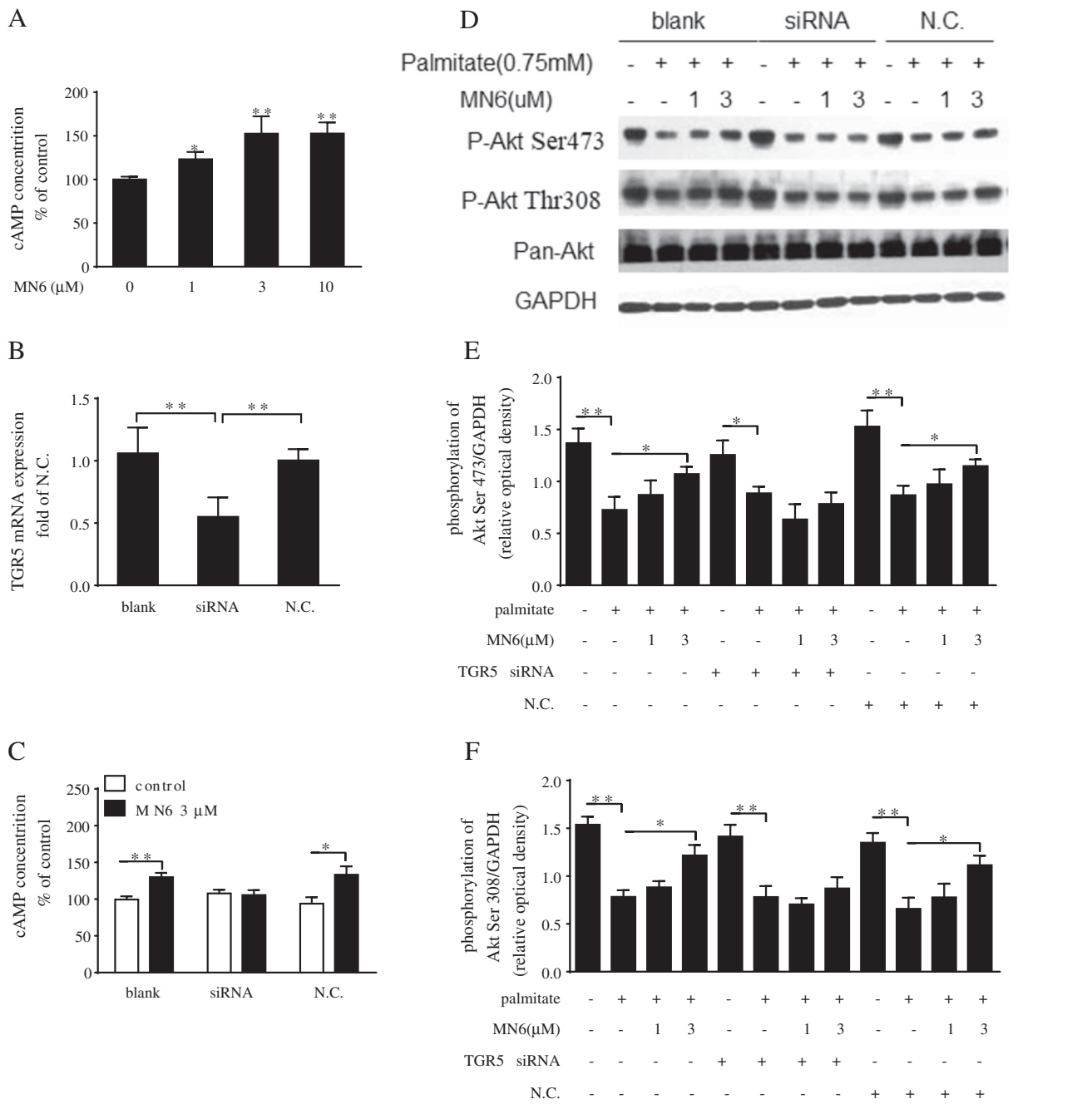

Fig. 5. TGR5 is indispensable in MN6's protection against palmitate-induced insulin resistance in C2C12 myotubes. (A) The cellular cAMP levels were measured in C2C12 cells after 1 h of treatment with MN6 at the indicated concentrations (n = 3). In the siRNA study, C2C12 myotubes were transfected twice on day 2 and day 4 of differentiation with siLentFect lipid (blank), scrambled siRNA (N.C.) or siRNAs directed against TGR5 (siRNA), followed by the examination of the TGR5 mRNA level (n = 5) (B), the cAMP level (n = 6) (C) and analysis of insulin-stimulated Akt phosphorylation (D). Quantitative measurements of Akt phosphorylation on serine 473 (E) or threonine 308 (F) relative to those of GAPDH were calculated (n = 5). The results are presented as the means ± SEMs. $^{*}P < 0.05$, $^{**}P < 0.01$ versus the corresponding controls or as indicated.

against palmitate-induced insulin resistance. The effects of the AC inhibitor MDL-12330-A and the PKA inhibitor H89 on MN6 prevented Akt phosphorylation under the insulin-stimulated conditions were observed in C2C12 myotubes. As shown in Fig. 6A–C, the effects of MN6 on insulin-stimulated Akt phosphorylation (Ser 473 and Thr 308) were completely blocked by MDL-12330-A in C2C12 myotubes. The improvement of insulin-stimulated Akt phosphorylation by MN6 was also completely blocked by H89 pretreatment (Fig. 6D–F), suggesting that MN6 prevented palmitate-induced insulin resistance in a manner that was dependent on the elevated cAMP level and PKA activation.

3.7. LCA prevented palmitate-induced insulin resistance in C2C12 myotubes

To test whether the native agonist of TGR5 has the same function as MN6, we treated C2C12 myotubes with LCA in the same way as we treated MN6. Preincubation with 3 μM LCA prevented the palmitate-induced impairment of insulin-stimulated Akt phosphorylation (Fig. 7A and B). LCA (10 μM) significantly ameliorated the palmitate-induced decrease in insulin-stimulated glycogen synthesis (Fig. 7C). Thus, we speculated that LCA, the natural agonist of TGR5, had similar functions as those of MN6 in preventing palmitate-induced insulin resistance.

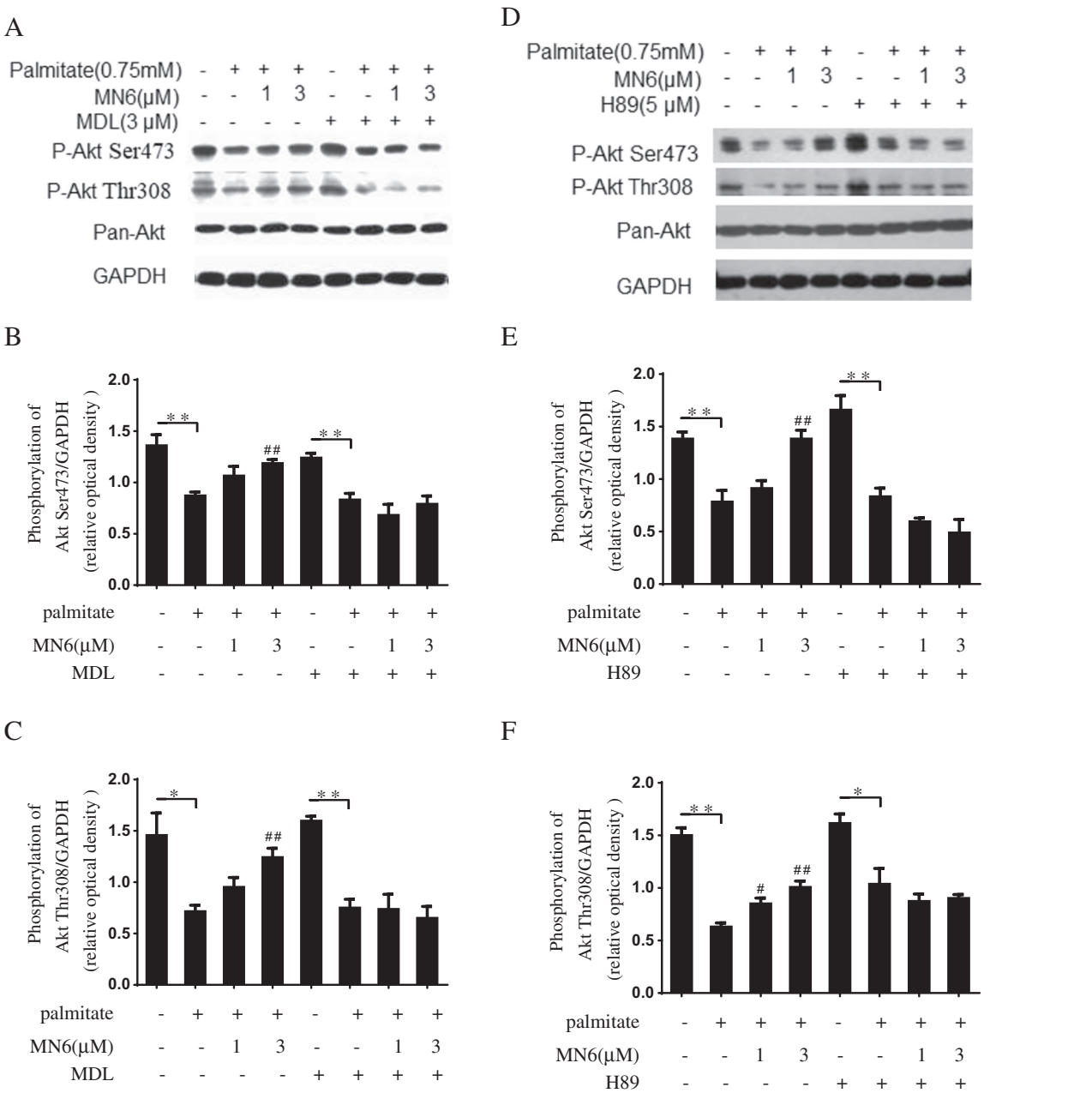

Fig. 6. Activation of TGR5 by MN6 prevented palmitate-induced insulin resistance via the cAMP/PKA pathway in C2C12 myotubes. C2C12 myotubes were treated with MN6 at the indicated concentrations for 8 h prior to coincubation with 0.75 mM palmitate for 16 h, supplemented with or without 3 μM MDL-12330-A (n = 4) (A-C) or 5 μmol/L H89 (n = 5) (D-F), followed by stimulation with 10 nM insulin for 30 min. Quantitative measurements of Akt phosphorylation on serine 473 or threonine 308 relative to those of GAPDH were calculated. The results are presented as the means ± SEMs. $^{*}P < 0.05$, $^{**}P < 0.01$ versus the corresponding controls or as indicated; $^{\#}P < 0.05$, $^{\#\#}P < 0.01$ versus the palmitate-treated group.

4. Discussion

The activation of TGR5 greatly impacts many physiological functions [5,32,33]; however, whether the TGR5 agonist could directly ameliorate insulin resistance and regulate glucose metabolism in the skeletal muscles has not been fully elucidated. In the current study, we demonstrated that MN6, a potent TGR5 agonist, stimulated GLP-1 secretion, ameliorated hyperglycemia in diabetic mice, and improved glucose and insulin tolerance in DIO mice. More importantly, our study shows that MN6 enhanced insulin-stimulated glucose transport in the skeletal muscles of DIO mice and prevented the palmitate-induced impairment of insulin-stimulated Akt phosphorylation, glucose uptake and glycogen synthesis in C2C12 myotubes. The preventative effect of MN6 on palmitate-induced insulin resistance in C2C12 myotubes was dependent on the activation of TGR5 and the cAMP/PKA pathway.

In recent years, developing small molecular agonists of TGR5 has become a hot spot in drug discovery for its promising potential in treating metabolic syndromes [11,25,26,34]. Among the reported agonists, MN6 showed outstanding efficacy toward TGR5 (EC_{50} values of 1.5 and 18 nM on hTGR5 and mTGR5, respectively) compared to the efficacy of other synthetic agonists, such as INT-777 (EC_{50} value was 820 nM on hTGR5) and INT-767 (EC_{50} value was 630 nM on hTGR5) [35,36]; in addition MN6 did not have FXR activity. TGR5 agonists were reported to increase the cellular cAMP levels, stimulating GLP-1 secretion from intestinal L-cells and, thus, regulating glucose homeostasis [6,37,38]. Here, MN6 increased cAMP production in human TGR5- and mouse

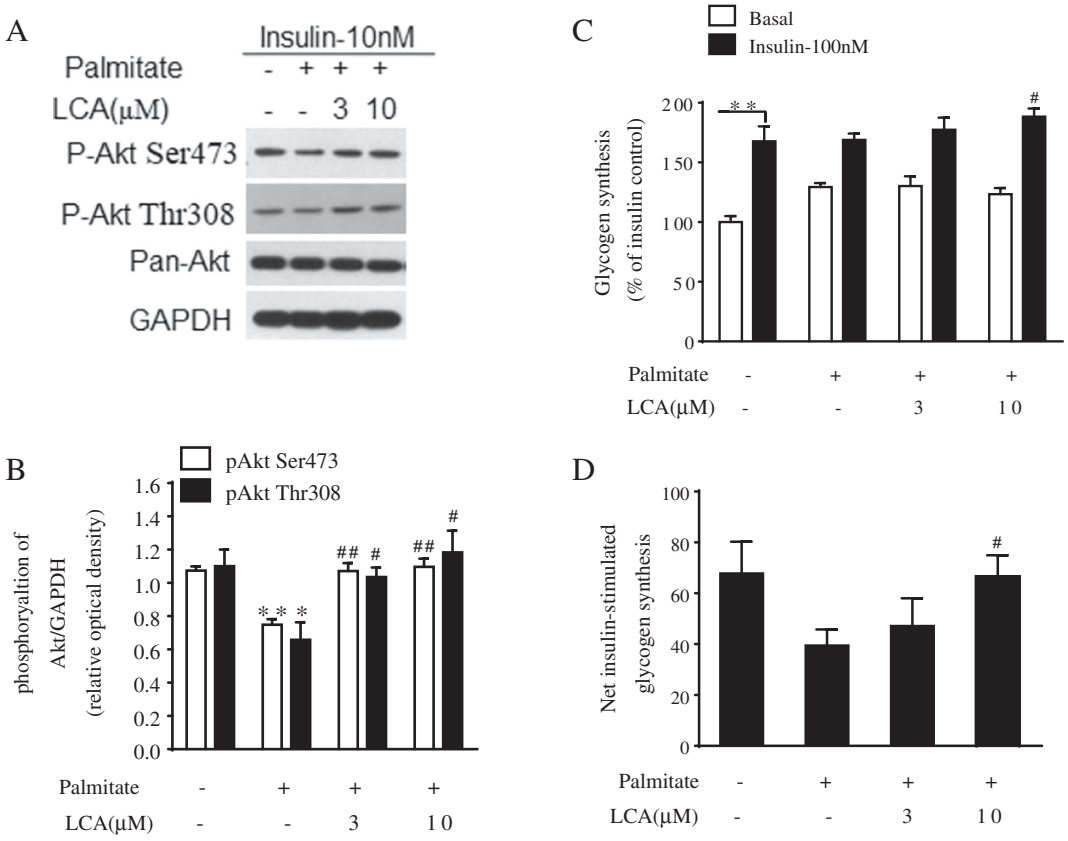

Fig. 7. LCA prevented palmitate-induced insulin resistance in C2C12 myotubes. (A, B) The effects of LCA on palmitate-attenuated insulin-stimulated phospho-Akt levels were detected in C2C12 myotubes. (n = 5). (C, D) The effects of LCA on glycogen synthesis and the levels of net insulin-stimulated glycogen synthesis (n = 3). The myotubes were treated, and the experiments were performed as described in Fig. 4. The results are presented as the means ± SEMs. $^{*}P < 0.05$, $^{**}P < 0.01$ versus the control group or as indicated; $^{\#}P < 0.05$ versus the palmitate-treated group.

TGR5-overexpressing HEK293 cells; this is consistent with our results from a previous report where we had performed a CRE-driven luciferase reporter gene assay [26]. As expected, MN6 stimulated GLP-1 secretion both in NCI-H716 cells and in CD1 mice; in addition, MN6 showed a pronounced effect when co-administered with the DPP-4 inhibitor BI-1356. Moreover, the efficacy studies show that a single dose of MN6 significantly decreased the blood glucose levels of *ob*/*ob* mice, and 15 days of treatment with MN6 reduced the fasting blood glucose level and the HbA1c level in *ob*/*ob* mice, proving the potency of MN6 in treating hyperglycemia by acting as a TGR5 agonist.

DIO mice are clinically relevant models of diabesity and are similar to obese humans who consume high-fat and energy-rich diets. After HFD treatment, the mice developed obesity and showed a greater insulin resistance that determined by the glucose tolerance test and the insulin tolerance test compared to the respective tolerances in the SD mice. Here, MN6 administration significantly ameliorated both glucose tolerance and insulin tolerance, indicating an improvement in insulin sensitivity, which is in accordance with results obtained in the INT777-treated DIO mice [6]. It was well demonstrated that GLP-1 agonists regulate appetite and cause weight loss [39]. The food intake and body weight of DIO mice were decreased by MN6 treatment, it might be caused by TGR5 mediating stimulation of GLP-1 secretion. The limitation of our current study is that we did not set a pair feeding control to exclude the affection of food intake. However, these changes on food intake and body weight were not found in the study on *ob*/*ob* mice. The plausible explanation for the differences might lie with the different animal models. Unlike the modified GLP-1 peptide, the native GLP-1 release stimulated by TGR5 activation would be quickly degraded by DPP-4. A report showed that plasma DPP-4 activity of leptin-deficient *ob*/*ob* mice was significantly higher than non-diabetic mice [40], which might be the reason of the lack of effects of MN6 on food intake and body weight in *ob*/*ob* mice. INT777 was shown to increase insulin-stimulated glucose uptake in the muscles of DIO mice after 10 weeks of treatment, but no further investigation was performed to evaluate whether any direct effects that are independent of GLP-1 may be involved [6,41]. Our results show that treatment with MN6 for 39 days increased the insulin-stimulated glucose transport in the skeletal muscles of DIO mice, indicating that there was an improvement in the glucose metabolism of the skeletal muscles. TGR5 was reported to play important roles in modulating some signaling pathways that were associated with insulin signaling, such as nuclear factor-κB (NF-κB) in vascular endothelial cells [42] and the Akt signaling pathway in macrophages [43,44]. Therefore, we wondered whether the activation of TGR5 would have similar effects on the Akt signaling pathway, which would further regulate glucose utilization in the skeletal muscles, although the beneficial effects of MN6 on glucose homeostasis and insulin sensitivity may also be related to the increased levels of GLP-1 secretion. Thus, to evaluate the direct effects of TGR5 activation on glucose metabolism and insulin sensitivity in the skeletal muscles, we further investigated the regulatory effects of MN6 on palmitate-induced insulin resistance in C2C12 myotubes.

The elevation of free fatty acids may be a primary factor in the development of insulin resistance and may further result in a reduction in the levels of both glucose transport and glycogen synthesis in skeletal muscles [17,45]. Here, we used palmitate to induce insulin resistance in C2C12 myotubes. Pretreatment with MN6 antagonized palmitate-induced insulin resistance by ameliorating palmitate-impaired insulin-stimulated Akt phosphorylation, glucose uptake and glycogen synthesis

in C2C12 myotubes. As native ligands of TGR5, BAs have been widely used to explore the physiological functions and beneficial effects of TGR5 activation on metabolic disorders [3,5,6,46]. Here, LCA, a native BA, showed a high similarity to the effects of MN6 on Akt phosphorylation and glycogen synthesis, which further verified that TGR5 activation could counteract palmitate-induced insulin resistance in C2C12 myotubes.

TGR5 activation is known to directly trigger cAMP generation. Here, MN6 increased the cellular cAMP levels in C2C12 myotubes as it did in HEK293 cells transfected with a TGR5 expression plasmid. To investigate the role of TGR5 in mediating the effects of MN6 in the skeletal muscles, siRNA transfection and inhibition studies were performed in C2C12 myotubes. The effects of MN6 on cAMP generation and insulin-stimulated Akt phosphorylation were completely abolished upon the down-regulation of TGR5, indicating that these effects were dependent on TGR5. These results were further demonstrated by using the adenylate cyclase inhibitor MDL-12330-A, which inhibits intracellular cAMP generation. This AC inhibitor completely blocked the preventative effects of MN6 on insulin-stimulated Akt phosphorylation impaired by palmitate. Thus, the protective effect of MN6 on palmitate-induced insulin resistance is dependent on TGR5-stimulated cAMP generation in C2C12 myotubes.

The physiological effects of cAMP are mainly mediated by cAMP-dependent PKA, which in turn, phosphorylates and regulates the functions of downstream protein targets [47–49]. The effects of cAMP/PKA on glucose metabolism and insulin signaling have been controversial due to the use of different physiological conditions [50,51]. Mangmool's report shows that sustained βAR stimulation inhibited insulin-stimulated glucose uptake and GLUT4 translocation in a PKA-dependent manner in cardiomyocytes [50]. However, another study shows that a thyroid-stimulating hormone increased Akt phosphorylation and glucose uptake in L6 myotubes [52], suggesting that the selective activation of PKA in the skeletal muscles could be positively associated with insulin sensitivity. Here, using the PKA inhibitor H89 [53], we found that the preventive effects of MN6 on the palmitate-induced suppression of insulin-stimulated Akt phosphorylation in C2C12 myotubes was fully abolished, indicating that PKA activity was necessary. Taking these results together, we can conclude that the effects of MN6 on ameliorating insulin resistance in the skeletal muscles depends on TGR5 and cAMP/PKA pathway activation.

5. Conclusions

In this study, by using MN6, a potent and selective agonist of TGR5, we show the beneficial effects of TGR5 activation on the regulation of glucose homeostasis and insulin resistance. MN6 reduced the high levels of blood glucose in *ob*/*ob* mice, a genetic diabetic animal model, and improved the glucose tolerance and insulin tolerance in DIO mice. More importantly, this study demonstrates that MN6 increased the insulin-stimulated glucose transport in the skeletal muscles of DIO mice and that the activation of TGR5 could ameliorate palmitate-induced insulin resistance in C2C12 myotubes through the cAMP/PKA pathway. Although the GLP-1-mediated effects could not be excluded in the in vivo studies, we can ascertain that some direct effects of TGR5 activation in the skeletal muscles would contribute to the improvement in glucose homeostasis and insulin sensitivity based on the experiments in C2C12 myotubes. These results uncovered a new effect of TGR5 agonists on regulating insulin sensitivity in the skeletal muscles and further strengthened the potential value of TGR5 agonists for the treatment of type 2 diabetes.

Funding

This study was financially supported by the National Natural Science Foundation of China (No. 81202571).

Author contribution

YL, JS, and SH designed the research. SH, SM, MN, WY, YY, and LZ performed the research. SH, SM, MN and YL analyzed and interpreted the data. SH, SM and YL wrote the paper. All authors approved the final version of the manuscript to be published.

Declaration of Competing Interest

The authors have no conflicts of interest to declare.

Acknowledgment

We would like to acknowledge the help we received from Dr. Jia Liu and her staff for their help with the pharmacokinetic study.

Appendix A. Supplementary data

Supplementary data to this article can be found online at https://doi.org/10.1016/j.metabol.2019.07.003.

References

[1] Takaharu Maruyama YM. Takao Nakamura, Yoshitaka Tamai, Hiromasa Okada, Eiji Sugiyama, Tatsuji Nakamura, Hiraku Itadani, and Kenichi Tanaka*. Identification of membrane-type receptor for bile acids (M-BAR). BBRC 2002;298:714–9.
[2] Kawamata Y, Fujii R, Hosoya M, Harada M, Yoshida H, Miwa M, et al. A G protein-coupled receptor responsive to bile acids. J Biol Chem 2003;278:9435–40.
[3] Deutschmann K, Reich M, Klindt C, Droge C, Spomer L, Haussinger D, et al. Bile acid receptors in the biliary tree: TGR5 in physiology and disease. BBA-Mol Basis Dis 1864;2018:1319–25.
[4] Hogenauer K, Arista L, Schmiedeberg N, Werner G, Jaksche H, Bouhelal R, et al. G-protein-coupled bile acid receptor 1 (GPBAR1, TGR5) agonists reduce the production of proinflammatory cytokines and stabilize the alternative macrophage phenotype. J Med Chem 2014;57:10343–54.
[5] Watanabe M, Houten SM, Mataki C, Christoffolete MA, Kim BW, Sato H, et al. Bile acids induce energy expenditure by promoting intracellular thyroid hormone activation. Nature 2006;439:484–9.
[6] Thomas C, Gioiello A, Noriega L, Strehle A, Oury J, Rizzo G, et al. TGR5-mediated bile acid sensing controls glucose homeostasis. Cell Metab 2009;10:167–77.
[7] Parker HE, Wallis K, le Roux CW, Wong KY, Reimann F, Gribble FM. Molecular mechanisms underlying bile acid-stimulated glucagon-like peptide-1 secretion. Br J Pharmacol 2012;165:414–23.
[8] Zambad SP, Tuli D, Mathur A, Ghalsasi SA, Chaudhary AR, Deshpande S, et al. TRC210258, a novel TGR5 agonist, reduces glycemic and dyslipidemic cardiovascular risk in animal models of diabesity. Diabetes Metab Syndr Obesity Targets Ther 2013;7:1–14.
[9] Finn PD, Rodriguez D, Kohler J, Jiang Z, Wan S, Blanco E, et al. Intestinal TGR5 agonism improves hepatic steatosis and insulin sensitivity in Western diet-fed mice. Am J Physiol Gastrointest Liver Physiol 2019;316:412–24.
[10] Katsuma S, Hirasawa A, Tsujimoto G. Bile acids promote glucagon-like peptide-1 secretion through TGR5 in a murine enteroendocrine cell line STC-1. Biochem Biophys Res Commun 2005;329:386–90.
[11] Agarwal S, Sasane S, Kumar J, Deshmukh P, Bhayani H, Giri P, et al. Evaluation of novel TGR5 agonist in combination with Sitagliptin for possible treatment of type 2 diabetes. Bioorg Med Chem Lett 2018;28:1849–52.
[12] Briere DA, Bueno AB, Gunn EJ, Michael MD, Sloop KW. Mechanisms to elevate endogenous GLP-1 beyond injectable GLP-1 analogs and metabolic surgery. Diabetes 2018;67:309–20.
[13] Teodoro JS, Zouhar P, Flachs P, Bardova K, Janovska P, Gomes AP, et al. Enhancement of brown fat thermogenesis using chenodeoxycholic acid in mice. Int J Obes (Lond) 2014;38:1027–34.
[14] Brons C, Grunnet LG. MECHANISMS IN ENDOCRINOLOGY skeletal muscle lipotoxicity in insulin resistance and type 2 diabetes: a causal mechanism or an innocent bystander? Eur J Endocrinol 2017;176:R67–78.
[15] Wu HZ, Ballantyne CM. Skeletal muscle inflammation and insulin resistance in obesity. J Clin Investig 2017;127:43–54.
[16] Yang J. Enhanced skeletal muscle for effective glucose homeostasis. Prog Mol Biol Transl Sci 2014;121:133–63.
[17] Turner N, Cooney GJ, Kraegen EW, Bruce CR. Fatty acid metabolism, energy expenditure and insulin resistance in muscle. J Endocrinol 2014;220:T61–79.
[18] Czech MP. Insulin action and resistance in obesity and type 2 diabetes. Nat Med 2017;23:804–14.
[19] Ostergaard L, Frandsen CS, Madsbad S. Treatment potential of the GLP-1 receptor agonists in type 2 diabetes mellitus: a review. Expert Rev Clin Pharmacol 2016;9:241–65.
[20] Broeders EPM, Nascimento EBM, Havekes B, Brans B, Roumans KHM, Tailleux A, et al. The bile acid chenodeoxycholic acid increases human Brown adipose tissue activity. Cell Metab 2015;22:418–26.

[21] Sasaki T, Kuboyama A, Mita M, Murata S, Shimizu M, Inoue J, et al. The exercise-inducible bile acid receptor Tgr5 improves skeletal muscle function in mice. J Biol Chem 2018;293:10322–32.
[22] Zhu J, Ning M, Guo C, Zhang L, Pan G, Leng Y, et al. Design, synthesis and biological evaluation of a novel class of potent TGR5 agonists based on a 4-phenyl pyridine scaffold. Eur J Med Chem 2013;69:55–68.
[23] Zou Q, Duan H, Ning M, Liu J, Feng Y, Zhang L, et al. 4-Benzofuranyloxynicotinamide derivatives are novel potent and orally available TGR5 agonists. Eur J Med Chem 2014;82:1–15.
[24] Ma SY, Ning MM, Zou QA, Feng Y, Ye YL, Shen JH, et al. OL3, a novel low-absorbed TGR5 agonist with reduced side effects, lowered blood glucose via dual actions on TGR5 activation and DPP-4 inhibition. Acta Pharmacol Sin 2016;37:1359–69.
[25] Duan HL, Ning MM, Zou QA, Ye YL, Feng Y, Zhang LN, et al. Discovery of intestinal targeted TGR5 agonists for the treatment of type 2 diabetes. J Med Chem 2015;58:3315–28.
[26] Duan H, Ning M, Chen X, Zou Q, Zhang L, Feng Y, et al. Design, synthesis, and antidiabetic activity of 4-phenoxynicotinamide and 4-phenoxypyrimidine-5-carboxamide derivatives as potent and orally efficacious TGR5 agonists. J Med Chem 2012;55:10475–89.
[27] Surwit RS, Kuhn CM, Cochrane C, McCubbin JA, Feinglos MN. Diet-induced type II diabetes in C57BL/6J mice. Diabetes 1988;37:1163–7.
[28] Haluzik M, Colombo C, Gavrilova O, Chua S, Wolf N, Chen M, et al. Genetic background (C57BL/6J versus FVB/N) strongly influences the severity of diabetes and insulin resistance in ob/ob mice. Endocrinology 2004;145:3258–64.
[29] Huang SL, Yu RT, Gong J, Feng Y, Dai YL, Hu F, et al. Arctigenin, a natural compound, activates AMP-activated protein kinase via inhibition of mitochondria complex I and ameliorates metabolic disorders in ob/ob mice. Diabetologia 2012;55:1469–81.
[30] Pirkmajer S, Kulkarni SS, Tom RZ, Ross FA, Hawley SA, Hardie DG, et al. Methotrexate promotes glucose uptake and lipid oxidation in skeletal muscle via AMPK activation. Diabetes 2015;64:360–9.
[31] Miklosz A, Lukaszuk B, Baranowski M, Gorski J, Chabowski A. Effects of inhibition of serine palmitoyltransferase (SPT) and sphingosine kinase 1 (SphK1) on palmitate induced insulin resistance in L6 myotubes. PloS one 2013;8.
[32] Hodge RJ, Nunez DJ. Therapeutic potential of Takeda-G-protein-receptor-5 (TGR5) agonists. Hope or hype? Diabetes Obes Metab 2016;18:439–43.
[33] Biagioli M, Cipriani S, Sorcini D, Carino A, Marchiano S, Zampella A, et al. Gpbar1 (Tgr5) ligation protects against colitis development by regulating leukocyte traffinking and promoting a Il-10 dependent shift in the M1/M2 phenotype. Gastroenterology 2017;152:S135-S.
[34] Yu DD, Sousa KM, Mattern DL, Wagner J, Fu X, Vaidehi N, et al. Stereoselective synthesis, biological evaluation, and modeling of novel bile acid-derived G-protein coupled Bile acid receptor 1 (GP-BAR1, TGR5) agonists. Bioorg Med Chem 2015;23:1613–28.
[35] Pellicciari R, Gioiello A, Macchiarulo A, Thomas C, Rosatelli E, Natalini B, et al. Discovery of 6alpha-ethyl-23(S)-methylcholic acid (S-EMCA, INT-777) as a potent and selective agonist for the TGR5 receptor, a novel target for diabesity. J Med Chem 2009;52:7958–61.
[36] Rizzo G, Passeri D, De Franco F, Ciaccioli G, Donadio L, Rizzo G, et al. Functional characterization of the semisynthetic bile acid derivative INT-767, a dual Farnesoid X receptor and TGR5 agonist. Mol Pharmacol 2010;78:617–30.
[37] Potthoff MJ, Potts A, He TT, Duarte JAG, Taussig R, Mangelsdorf DJ, et al. Colesevelam suppresses hepatic glycogenolysis by TGR5-mediated induction of GLP-1 action in DIO mice. Am. J. Phys. Gastrointest. Liver 2013;304:G371-G80.
[38] Ono E, Inoue J, Hashidume T, Shimizu M, Sato R. Anti-obesity and anti-hyperglycemic effects of the dietary citrus limonoid nomilin in mice fed a high-fat diet. Biochem Biophys Res Commun 2011;410:677–81.
[39] van Bloemendaal L, IJ RG, Ten Kulve JS, Barkhof F, Konrad RJ, Drent ML, et al. GLP-1 receptor activation modulates appetite- and reward-related brain areas in humans. Diabetes 2014;63:4186–96.
[40] Yusuke Moritoh KT. Tomoko Asakawa, Osamu Kataoka, Hiroyuki Odaka. Chronic administration of alogliptin, a novel, potent, and highly selective dipeptidyl peptidase-4 inhibitor, improves glycemic control and beta-cell function in obese diabetic ob/ob mice. Eur J Pharmacol 2008;588:325–32.
[41] Vallim TQ, Edwards PA. Bile acids have the gall to function as hormones. Cell Metab 2009;10:162–4.
[42] Kida T, Tsubosaka Y, Hori M, Ozaki H, Murata T. Bile acid receptor TGR5 agonism induces NO production and reduces monocyte adhesion in vascular endothelial cells. Arterioscler Thromb Vasc Biol 2013;33:1663–9.
[43] Perino A, Pols TW, Nomura M, Stein S, Pellicciari R, Schoonjans K. TGR5 reduces macrophage migration through mTOR-induced C/EBPbeta differential translation. J Clin Invest 2014;124:5424–36.
[44] Yanguas-Casas N, Barreda-Manso MA, Nieto-Sampedro M, Romero-Ramirez L. TUDCA: an agonist of the bile acid receptor GPBAR1/TGR5 with anti-inflammatory effects in microglial cells. J Cell Physiol 2017;232:2231–45.
[45] GdP Antonia Giacco, Senese Rosalba, Cioffi Federica, Silvestri Elena, Moreno Maria, Ruoppolo Margherita, et al. The saturation degree of fatty acids and their derived acylcarnitines determines the direct effect of metabolically active thyroid hormones on insulin sensitivity in skeletal muscle cells. FASEB J 2018;33:1811–23 (Sep 11:: fj201800724R).
[46] van Nierop FS, de Jonge C, Kulik W, Bouvy N, Schaap FG, Olde Damink SW, et al. Duodenal-jejunal lining increases postprandial unconjugated bile acid responses and disrupts the bile acid-FXR-FGF19 axis in humans. Metab Clin Exp 2019;93:25–32.
[47] Dong ZH, Chai WD, Wang WH, Zhao LN, Fu Z, Cao WH, et al. Protein kinase A mediates glucagon-like peptide 1-induced nitric oxide production and muscle microvascular recruitment. Am. J. Physiol. Endocrinol. Metab. 2013;304:E222-E8.
[48] Hewer RC, Sala-Newby GB, Wu YJ, Newby AC, Bond M. PKA and Epac synergistically inhibit smooth muscle cell proliferation. J Mol Cell Cardiol 2011;50:87–98.
[49] Alkhateeb H, Qnais E. Preventive effect of oleate on palmitate-induced insulin resistance in skeletal muscle and its mechanism of action. J Physiol Biochem 2017;73:605–12.
[50] Mangmool S, Denkaew T, Phosri S, Pinthong D, Parichatikanond W, Shimauchi T, et al. Sustained betaAR stimulation mediates cardiac insulin resistance in a PKA-dependent manner. Mol Endocrinol 2016;30:118–32.
[51] Ngala Robert A, O'Dowd Jacqueline F, Stocker Claire J, Cawthorne Michael A, Arch Jonathan RS. β2-adrenoceptor agonists can both stimulate and inhibit glucose uptake in mouse soleus muscle through ligand-directed signalling. Naunyn Schmiedebergs Arch Pharmacol 2013;386:761–73.
[52] Moon MK, Kang GH, Kim HH, Han SK, Do Koo Y, Cho SW, et al. Thyroid-stimulating hormone improves insulin sensitivity in skeletal muscle cells via cAMP/PKA/CREB pathway-dependent upregulation of insulin receptor substrate-1 expression. Mol Cell Endocrinol 2016;436:50–8.
[53] Chijiwa T, Mishima A, Hagiwara M, Sano M, Hayashi K, Inoue T, et al. Inhibition of forskolin-induced neurite outgrowth and protein phosphorylation by a newly synthesized selective inhibitor of cyclic AMP-dependent protein kinase, N-[2-(p-bromocinnamylamino)ethyl]-5-isoquinolinesulfonamide (H-89), of PC12D pheochromocytoma cells. J Biol Chem 1990;265:5267–72.